P-selectin deficiency attenuates tumor growth and metastasis

Young J. Kim, Lubor Borsig, Nissi M. Varki, and Ajit Varki

This information is current as of March 2007.

Notes:

P-selectin deficiency attenuates tumor growth and metastasis

(mucins/cancer/carbohydrates/lectin/Lewis antigens)

Young J. Kim, Lubor Borsig, Nissi M. Varki, and Ajit Varki*

Glycobiology Program and University of California at San Diego Cancer Center, Divisions of Hematology–Oncology and Cellular and Molecular Medicine, University of California at San Diego, La Jolla, CA 92093

ABSTRACT Selectins are adhesion receptors that normally recognize certain vascular mucin-type glycoproteins bearing the carbohydrate structure sialyl-Lewis[x]. The clinical prognosis and metastatic progression of many epithelial carcinomas has been correlated independently with production of tumor mucins and with enhanced expression of sialyl-Lewis[x]. Metastasis is thought to involve the formation of tumor-platelet-leukocyte emboli and their interactions with the endothelium of distant organs. We provide a link between these observations by showing that P-selectin, which normally binds leukocyte ligands, can promote tumor growth and facilitate the metastatic seeding of a mucin-producing carcinoma. P-selectin-deficient mice showed significantly slower growth of subcutaneously implanted human colon carcinoma cells and generated fewer lung metastases from intravenously injected cells. Three potential pathophysiological mechanisms are demonstrated: first, intravenously injected tumor cells home to the lungs of P-selectin deficient mice at a lower rate; second, P-selectin-deficient mouse platelets fail to adhere to tumor cell-surface mucins; and third, tumor cells lodged in lung vasculature after intravenous injection often are decorated with platelet clumps, and these are markedly diminished in P-selectin-deficient animals.

Most human cancers are of epithelial origin, and most deaths resulting from such carcinomas are caused by tumor spread to distant organs (metastasis). Metastasis is a multistep cascade involving many factors favoring survival of the "fittest" cells that enter the bloodstream, successfully evade host defenses, bind to the endothelium of distant organs, and invade and colonize these sites (1–3). Substantial evidence indicates that platelets and leukocytes interact with hematogenously borne tumors cells, which are thought to create tumor microemboli, facilitating arrest in distant organs and subsequent interactions with endothelial cells (3–5). A reduction in circulating platelets can reduce experimental metastasis in mice (3, 4), and the relevant platelet interactions seem to involve carcinoma cell-surface glycoproteins (3, 5, 6). The molecular basis of these proposed tumor cell–platelet interactions remain largely unexplained.

Alteration of cell-surface carbohydrates is a universal phenotype of cancer cells (7–13). Cancer sialomucins are large anionic molecules thought to act as antiadhesins, preventing cell–cell interactions, e.g., with host cytotoxic cells (14–16). Inhibition of cancer sialomucin O-glycosylation can diminish metastasis formation in mouse models (11, 17). Among the carcinoma-associated glycans, the expression of sialyl Lewis[x] (sLe[x]) and sialyl Lewis[a] (sLe[a]) consistently correlates with tumor progression, metastatic spread, and poor prognosis (18–27).

The selectins are well characterized vascular receptors for certain sLe[x/a]-containing, mucin-type glycoproteins (28–33). P-selectin expressed on activated endothelium tethers PSGL-1 on leukocytes under flow conditions, initiating rolling, and eventually resulting in leukocyte arrest on the endothelium. L-selectin on other leukocytes can also interact with PSGL-1 on such arrested cells and/or with appropriately glycosylated ligands on the endothelium (30–32). P-selectin on activated platelets also can mediate interactions with monocytes, initiating paracrine-signaling mechanisms amplifying inflammatory processes, as well as inducing tissue factor secretion, thus triggering thrombosis. E-selectin expression on endothelial cells is induced hours after initiation of inflammation and sustains leukocyte recruitment. Various lines of evidence indicate that sLe[x/a] oligosaccharides are essential for generating most normal selectin ligands (29–33). However, these glycans themselves are not sufficient for high-affinity recognition. For example, PSGL-1 cannot function as an L- or P-selectin ligand, unless the apomucin backbone has sLe[x]-bearing chains in close proximity to a cluster of sulfated tyrosine residues.

Because sLe[x/a] structures also are commonly expressed on carcinoma cells and are associated with poor clinical prognosis, investigators initially hypothesized that E-selectin expressed on endothelium might mediate the seeding of cancer cells into metastatic sites (25, 34–36). Indeed, many human colon cancer tissues and cells do express potential E-selectin ligands (37), and artificial overexpression of E-selectin in the liver of transgenic mice redirected the metastases of tumor cells that normally colonize the lung (38). However, this hypothesis does not include a role for platelets or leukocytes. P-selectin is a more logical candidate to mediate multiple interactions involving platelets, leukocytes, endothelium, and carcinoma cells, including the microthrombi and microemboli characteristic of mucin-producing carcinomas (3, 4). Indeed, P-selectin ligands have been detected on several human carcinomas and cell lines (37, 39, 40) and are suggested to play a role in metastasis. However, there has been no *in vivo* confirmation of a pathophysiological role for P-selectin in cancer biology. Here, we have generated P-selectin-deficient mice in a Rag2 −/− background, allowing the study of the role of P-selectin in tumor growth and metastasis.

MATERIALS AND METHODS

Production and Characterization of P-Selectin:Rag2 Double Null Mice. Female Rag2 −/− mice (41) in a 129 background (Taconic) were mated with male P-selectin −/− mice (42) in a C57/Bl background (The Jackson Laboratory). F1s were crossed and their offspring were genotyped for Rag2 null mutants and P-selectin −/− null mutants. For Rag2 genotyping, rag2a—GGGAGGACACTCACTTGCCAGTA, rag2b—

AGTCAGGAGTCTCCATCTCACTGA, and neoA—CG-GCCGGAGAACCTGCGTGCAA were used as primers in PCR at 55°C annealing temperature (43). For P-selectin, genotyping psela—TTGTAAATCAGAAGGAAGTGG, pselb—AGAGTTACTCTTGATGTAGATCTCC, and neoB—CACGAGACTAGTGAGACGTG were used (42), at 60°C annealing temperature. Double null mutants were backcrossed to Rag2 −/− mice in 129/J background and their F1 offspring were crossed against each other to generate double null animals in a predominantly 129/J background. Control Rag2 −/− mice were generated similarly from F1 generations. Double null mice were phenotyped for mature lymphocytes in peripheral blood by staining with phycoerythrin-conjugated anti-CD4- or anti-CD8-antibodies (Caltag, South San Francisco, CA) and analysis in a FACScan (Becton Dickinson), with appropriate controls. Frozen sections of lung tissues were fixed in formalin, blocked with 10% goat serum/1% BSA in PBS, and incubated with biotinylated anti-mouse P-selectin antibody (PharMingen) at 5 μg/ml in PBS/1% BSA for 1 hr, followed with streptavidin-peroxidase at 1 μg/ml in PBS/1% BSA for 30 min. Conjugates were detected with metal-enhanced diaminobenzidine tetrahydrochloride substrate (Pierce).

Tumor Growth Assays and Survival Curves. The human colon cancer cell lines LS180 and T-84 were passaged in αMEM media with 10% FCS. Cells (1 × 10⁶) were detached with 5 mM EDTA/PBS, disaggregated into single-cell suspensions, and injected s.c. into the lower flanks of 6- to 7-week-old mice, which were kept in a pathogen-free environment with antibiotics in their water. Tumors were measured along the plane of the body cavity and tumor volume was calculated as: $[(\text{length}) \times (\text{width})^2]/2$. The mice were followed for up to 2 months, when the largest tumor masses exceeded 20 cm³, and euthanasia was required by institutional guidelines. Paraffin-embedded sections of some tumors were blocked for nonspecific binding with 10% goat serum/1% BSA and incubated with biotinylated human P-selectin-Fc chimera in 20 mM Hepes/140 mM NaCl/5 mM CaCl₂ or 5 mM EDTA. Streptavidin-peroxidase was used as secondary probe as above.

Experimental Metastasis Assays. LS180 cells were detached with 5 mM EDTA and disaggregated in PBS. Persistent cell aggregates settled down within minutes, and single cells remaining in the supernatant (100,000) were injected into the tail vein. After 4 weeks, the mice were sacrificed, and their brains, lungs, livers, kidneys, and enlarged dorsal lumps were collected for analysis. Half of the tissue sample was analyzed histologically for metastasis, and the other half was subjected to human DNA analysis.

Micrometasis Detection Assay. This was done by a PCR-based modification of the previously reported method (44). Homogenized tissue samples were proteolyzed with proteinase K overnight, and total genomic DNA was extracted with phenol:choroform. Ethanol-precipitated DNA was resuspended in TE buffer, and the DNA/protein ratio was followed with a 260/280 ratio. If necessary, samples were reproteolyzed and reextracted. A final DNA purification was done with QiaAmp Tissue kit (Qiagen). Aliquots (500 μg) of DNA were amplified with human-specific Alu primer, GAGC-CGAGATCGCGCCACTGCACTCCAGCCTGGG, that has been used previously for fluorescence *in situ* hybridization analysis of human yeast artificial chromosome clones (45). The PCRs cycled 35 times at 95°C for 1 min and at 72°C for 2 min. PCR products analyzed in agarose gel electrophoresis showed prominent smears between 500 bp and 2 kb. Using genomic DNA prepared from LS180 cells, ≈100 fg of human DNA was detectable in the presence of 1 μg of mouse DNA. Primers for a mouse lysosomal sialic acid esterase were used in a control PCR to ensure that equal amounts of DNA were used. PCR products were quantified by blotting onto Hybond-N nylon membranes (Amersham) and probed with an end-labeled probe that hybridized within the Alu consensus region but did not overlap the primer used for PCR. This sequence is CCGAATTCGCCTCCCAAAGTGCTGGGATTACAG (45). Bound probe was detected and analyzed with a PhosphorImager (Molecular Dynamics). Genomic DNA of mice that did not receive an injection served as background controls.

Tumor Seeding Assay. LS180 cells were metabolically radiolabeled with [³H]thymidine and harvested into single-cell suspensions, and 500,000 cells (≈300,000 cpm) were injected into the tail vein. After 3 hr, the mice were sacrificed, blood was drained via cardiac puncture, and various organs were homogenized in 1% Triton/PBS solution with a Polytron. The samples were freeze-thawed several times, and an aliquot was digested extensively with proteinase K and counted in Eco-Scint scintillation cocktail.

Adherence of Platelets to Tumor Cells. Tail vein blood was collected into 1/10 volume of acid-citrate-dextrose (ACD, 38 mM citric acid/75 mM trisodium citrate/100 mM dextrose) and platelet-rich plasma (PRP) was obtained by centrifugation at 200 g for 20 min. Platelets were washed and labeled with 5 μM calcein AM (Molecular Probes) in PSG buffer (5 mM Pipes, pH 6.8/145 mM NaCl/4 mM KCl/0.5 mM sodium phosphate/5.5 mM glucose/0.5% BSA) while centrifuging at $500 \times g$ for 20 min. Platelets were rewashed with PSG buffer and gently resuspended in Hanks' balanced salt solution (HBSS, Sigma). LS180 cells were grown to 50% confluency in six-well plates (Falcon), washed twice with HBSS, and incubated with calcein-labeled platelets (3 × 10⁶ platelets per well) in the presence/absence of 1 mM of EDTA or 0.2 units of human thrombin. Some LS180 cells also were treated with *O*-sialoglycoprotein endopeptidase (OSGPase, Accurate Chemicals) before adding the platelets. After 15 min at room temperature (RT) with shaking, wells were washed twice with HBSS, fixed in formalin/PBS for 20 min, and washed with PBS. Calcein-stained platelets were visualized by fluorescence at 530 nm, and phase-contrast microscopy was used to visualize the LS180 cells.

***In Vivo* Interactions of Intravenously Injected Tumor Cells with Endogenous Platelets.** LS180 cells were grown to 80% confluency, washed with PBS, detached in PBS with 2 mM EDTA, washed and stained with 5 μM calcein AM (Molecular Probes) in PBS for 20 min, washed twice again in PBS, and resuspended in PBS for a final concentration of 3 × 10⁶ cells/ml. Anesthetized mice were injected intravenously with 60 μl of labeled LS180 cells. Blood was collected by retroorbital bleeding after 10 min (L eye) and 20 min (R eye) and immediately smeared on coverslips or fixed in 10% formalin. Mice were euthanized 30 min after injection. To prevent lung collapse, the trachea was clamped before opening the chest and the blood vessels and bronchi at the hilum were clamped soon thereafter. Lungs were dissected, immediately fixed in 10% formalin, and frozen. Freshly cut frozen lung sections were fixed in acetone for 10 min at RT, blocked with 10% goat serum/1% BSA in PBS, and stained with rat anti-mouse CD41 antibody (PharMingen) in 1:50 dilution for 30 min at RT. After washing with PBS, biotinylated goat anti-rat antibody (1:100 dilution) was added for 30 min at RT. After washing again with PBS, streptavidin R-phycoerythrin (1:100) was added for 30 min at RT, and the sections were washed in PBS, mounted, and analyzed by fluorescence microscopy.

RESULTS

Generation of P-Selectin Deficiency in Rag2 Null Mutants. All previously characterized colon carcinoma lines expressing SLeˣ/ᵃ and P-selectin ligands are of human origin. To study these cells in a model system, it is necessary to use immunodeficient mice that can accept transplanted human cells. We chose Rag2 −/− mice rather than nude mice, because the defect causes a specific deficiency of mature lymphocytes (41)

without directly affecting other tissues. Because the Rag2 and P-selectin genes are on separate chromosomes and both null mice are fertile, double null mutants and control P-selectin $+/+$ Rag2 $-/-$ mice were obtained by mating as described in *Materials and Methods* (Fig. 1*A*). These animals showed an absence of peripheral CD4$^+$ and CD8$^+$ lymphocytes (Fig. 1*B*) and an absence of P-selectin on lung endothelium (Fig. 1*C*). The mice were viable, with no gross defects, and appeared healthy when housed in a specific pathogen-free environment with controls.

Absence of P-Selectin Slows the Rate of Tumor Growth. LS180 colon carcinoma cells that express potential ligands for all three selectins (37) were used for xenotransplantation. Initial studies in Rag2 $-/-$ mice showed that $\approx 10^6$ s.c. injected cells became a palpable tumor within 2 weeks and grew rapidly in size thereafter. We next studied groups of 6- to 7-week-old Rag2 $-/-$ mice that were either wild-type or null for P-selectin (Fig. 2*A*). Tumor growth rate was reduced significantly in the absence of P-selectin. Occasional tumors in P-selectin null mice even showed regression and regrowth (data not shown). Histologically, there were no obvious differences in general appearance, extent of vascularization, or the level of infiltrating neutrophils and mononuclear cells (data not shown). P-selectin ligand expression in the tumors was confirmed by probing sectioned tissues with soluble recombinant P-selectin (data not shown). Prolonged follow-up was not possible because overall tumor bulk, weight loss, and occasional local ulceration exceeded institutional guidelines, requiring termination of the experiments. Statistically significant differences in tumor growth rates were demonstrated before the onset of any regression phenomena or any animal deaths (at 30 days, see Fig. 2*B*).

The timing of death of each mouse was not related to the size of the primary tumor. A trend toward improved survival was
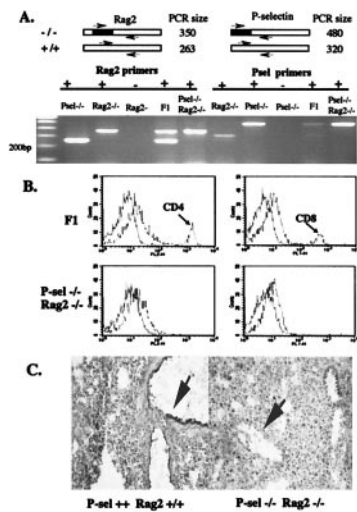

FIG. 1. Genotyping and phenotyping of P-selectin and Rag2 double null mutants. (*A*) Genomic DNA from mouse tail clips were used as templates for PCR genotype screening for Rag2 allele and P-selectin allele. The blackened region represents the neomycin A resistance gene that was targeted into both wild-type alleles; the arrows represent the two forward primers and the single reverse primer used in each reaction. Each PCR contained the three primers. F1 represents the double heterozygote from the first cross between Rag2 $-/-$ and P-selectin $-/-$ mice. (*B*) Peripheral blood from F1 mice and double null mutants was labeled with anti-CD4-phycoerythrin or anti-CD8-fluorescein isothiocyanate and analyzed by using a Becton Dickinson FACScan flow cytometer. (*C*) Frozen lung sections were probed with biotinylated anti-mouse P-selectin antibody and followed with streptavidin-peroxidase. The enzyme conjugate was detected with metal-enhanced diaminobenzidine substrate. The arrows indicate lung endothelium.
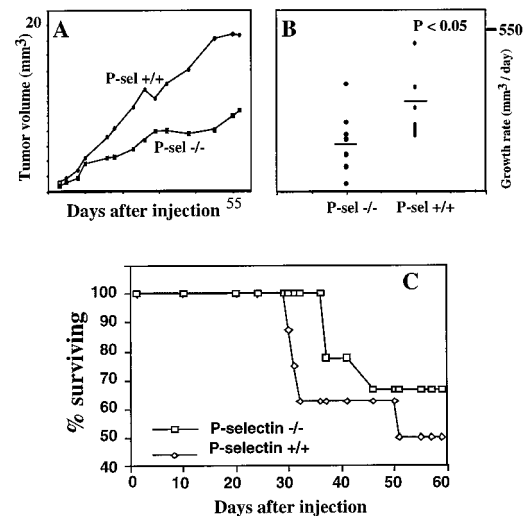

FIG. 2. Effects of P-selectin deficiency on primary tumor growth rate and survival. (*A*) The length and width of tumors arising from s.c. injected LS180 cells were measured and their volumes were calculated. Average tumor size for each mouse group ($n = 9$ per group) is plotted against time. (*B*) The growth rate at day 30 for each mouse was measured when all were still alive and was analyzed for statistical significance by using the Wilcoxon rank–sum test. The null hypothesis of equal ranks was rejected ($P < 0.05$). (*C*) Survival curve of mice with s.c. tumors ($n = 9$ per group). The trend toward improved survival did not achieve full statistical significance at 60 days, when institutional animal welfare guidelines required termination of the experiment.

seen in the P-selectin-deficient group (Fig. 2*C*), up to the point where some tumors reached a size requiring termination of the experiment to comply with institutional guidelines. At this point, the remaining mice were sacrificed and their lungs were examined. In general, the P-selectin $+/+$ mice appeared noticeably sicker than the P-selectin $-/-$ ones. Three independent observers noted that the wild-type mice were more cachetic, less mobile, and less well groomed than their mutant counterparts. The reason for this difference is unclear, but suggests that P-selectin affects some aspects of the biology of the cancer other than tumor size. Autopsies revealed direct peritoneal invasion in half of the mice; all the other organs looked grossly normal. Histological examination showed interstitial pneumonia in some animals of both groups, with metastatic tumor cells dispersed throughout the lung (data not shown). Occasional metastases also were visualized histologically in other organs, such as the liver, pancreas, and lymph nodes. Although there was a trend toward increased frequency of these metastases in the wild-type mice, the experiment could not be continued long enough to be certain (because of the rapid primary tumor growth rate in the wild-type animals, see above). Similar reductions in primary tumor growth rate also were seen with another colon carcinoma cell line, T-84, which expresses P-selectin ligands (ref. 37; data not shown).

P-Selectin Increases Experimental Micrometastasis to the Lung. Although the difference in primary tumor growth rate is interesting, it disallows testing of the original hypothesis regarding the role of P-selectin in metastasis (a decrease in primary tumor growth rate could reduce directly the rate of spontaneous metastasis). Therefore, we used intravenous ("experimental") metastasis assays. LS180 cells were injected intravenously into the tail vein of 6- to 7-week-old mice. After 4 weeks, most P-selectin $+/+$ mice (seven of nine) developed palpable lumps around the cervical area, both dorsally and ventrally, whereas only two of nine P-selectin $-/-$ mice developed similar masses. Generally, the wild-type mice also appeared sicker, with diminished grooming and mobility. Upon dissection, the masses were found to be enlarged lymph
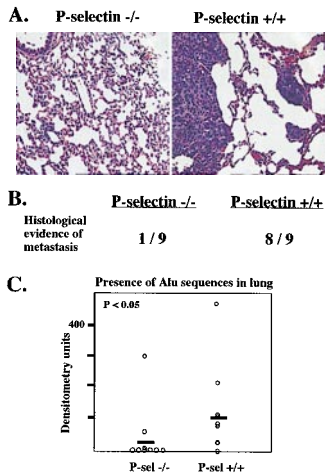
FIG. 3. P-selectin facilitates the development of micrometastasis in the lung. (*A*) LS180 cells were injected intravenously as described, and the mice were sacrificed after 4 weeks. Examples of hematoxylin/eosin-stained lung sections from each mouse type are shown. Note the micrometastasis evident in the P-selectin +/+ lung. (*B*) Several cross-sections of the lung from each mouse were analyzed for histological evidence of metastatic cells. (*C*) Micrometastases were quantitated by PCR analysis with primers for human *Alu* sequences as described in *Materials and Methods* and analyzed for statistical significance by using the Wilcoxon rank–sum test.

nodes containing tumor cells, or tumors growing within histologically undefined subcutaneous tissue. The lungs from both groups of mice showed some infiltrating macrophages, but no grossly visible metastatic nodules. However, in eight of nine P-selectin +/+ mice, scattered tumor cells and microscopic nodules were seen in the lung parenchyma (Fig. 3*A*), whereas only one P-selectin −/− mouse showed such histological evidence of metastasis (Fig. 3*B*). Other organs were not obviously affected.

To better quantitate the lung micrometastasis, the right lung from each mouse was homogenized and total genomic DNA
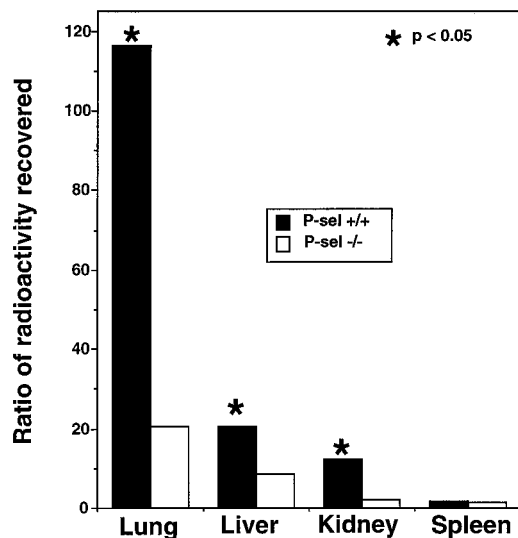
was purified and screened for the presence of human DNA using PCR primers that recognize human-specific *Alu* sequences (44). Lungs from uninjected mice were used as negative controls. PCR products were blotted onto membranes and probed with labeled oligonucleotides that hybridize to nested regions of the *Alu* PCR product. Signals quantified with a PhosphorImager showed that wild-type mice had significantly more human DNA in the lung than the P-selectin −/− counterparts, where only two specimens were even clearly positive (Fig. 3*C*). These results show that P-selectin is involved at some step in the colonization of hematogenously borne tumor cells into the lungs.

P-Selectin Facilitates the Initial Seeding of Metastatic Cells in the Lung. To explore the initial step of seeding of cells into the lung, LS180 cells were metabolically radiolabeled with [^{3}H]thymidine and injected as single-cell suspensions into the tail veins of mice. After 3 hr, various organs were collected and radioactivity was quantitated. In general, radioactivity in the lung and some other organs was decreased in P-selectin-deficient mice. Fig. 4 shows that the presence of P-selectin facilitates the selective accumulation of injected tumor cells into the lung and, to a lesser extent, into the liver and kidney. These data show that the initial seeding of hematogenous cells to a metastatic site can be at least partly P-selectin-dependent.

P-Selectin Mediates *in Vitro* Rosetting of Mouse Platelets with Tumor Cells via Cell-Surface Mucins. To explore whether P-selectin on mouse platelets has a role in the initial seeding of tumors cells to the lung, we labeled freshly isolated mouse platelets with calcein and applied them to the LS-180 cells *in vitro*. As seen in Fig. 5, wild-type platelets activated with

FIG. 4. P-selectin affects the seeding of intravenously injected tumor cells. Mice were injected with [^{3}H]thymidine-labeled LS180 cells. After 3 hr, tissues were homogenized and proteolyzed, and radioactivity was monitored, as described under *Materials and Methods*. To correct for differences in recovery of radioactivity per mouse, the results are shown as the ratios of radioactivity found in various organs relative to that found in the brain (which had 4–7% of the radioactivity in all mice). Residual radioactivity in the circulating blood was similar in both groups. Statistical significance values were generated by using Wilcoxon rank–sum test.
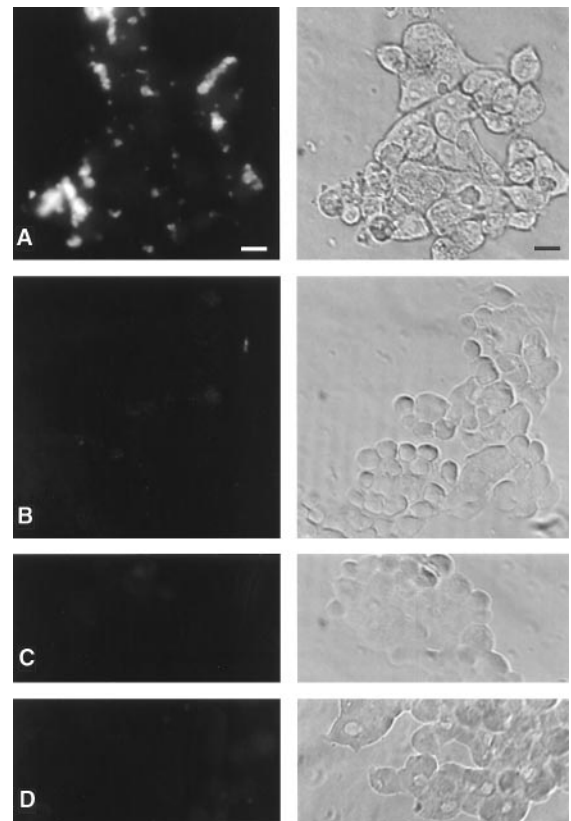

FIG. 5. P-selectin-deficient platelets fail to rosette on colon cancer cells in a calcium- and mucin-dependent manner. Calcein-labeled mouse platelets were studied for their interactions with cultured LS-180 cells as described in *Materials and Methods*. *Left*, fluorescence; *Right*, phase-contrast images. (*A*) P-selectin +/+ platelets. (*B*) P-selectin −/− platelets. (*C*) P-selectin +/+ platelets in 1 mM EDTA. (*D*) P-selectin +/+ platelets, tumor cells pretreated with OSGPase. (Bar = 50 µm.)

thrombin rosetted on the tumor cells, and this interaction was abolished by calcium chelation or by pretreatment of the tumor cells with OSGPase, which selectively cleaves mucins from the cell surfaces. Platelets from P-selectin-deficient mice do not show any rosetting, indicating that the mucin-dependent interaction is mediated primarily by P-selectin.

Optimal *in Vivo* Interactions of Tumors Cells with Platelets Requires P-Selectin. To examine these platelet:tumor cell interactions *in vivo*, we intravenously injected tumor cells (calcein-labeled or unlabeled) into mice and collected blood samples at 5, 10, 15, and 20 min postinjection. Although we detected some tumor cells remaining in the bloodstream (by fluorescence, or by Wright–Geimsa-stained blood smears), it was impossible to study their interaction with platelets. This is because all of the standard methods of anticoagulation (EDTA, citrate, or heparin) can themselves disrupt P-selectin-dependent interactions. We tried to make blood smears very rapidly after collection and/or to rapidly fix the blood cells in formaldehyde. However, in both cases, we were unable to avoid massive clumping of platelets that apparently was induced by the injury involved in the blood collection.

Therefore, we examined the tumor cells that were actually lodged in the blood vessels of the lung. Tumor cells (calcein-labeled or unlabeled) were injected intravenously, the mice were sacrificed at short time points postinjection, and the lungs were studied by frozen and/or paraffin-embedded sections. In the latter sections, unlabeled tumor cells were lodged in the capillaries of the lung, sometimes surrounded by fibrinous material (data not shown). However, the resolution was not sufficient to be certain that platelets were present in these complexes. Therefore, we obtained frozen sections of lungs after injection of calcein-labeled tumor cells and stained them with anti-CD41, a defined marker for platelets in the mouse. With this double-color-fluorescence approach, clumps of platelets could be seen attached to about half of the tumor cells in the lungs of wild-type mice. In about one-third of cases, the platelets were present in very large clumps that almost covered the tumor cells (see Fig. 6 for an example). In contrast, platelets rarely were associated with the tumor cells in the lungs of P-selectin-deficient mice ($\approx$10% of cells). Even when found, these did not consist of the heavy clumps seen in many of the wild-type lungs.
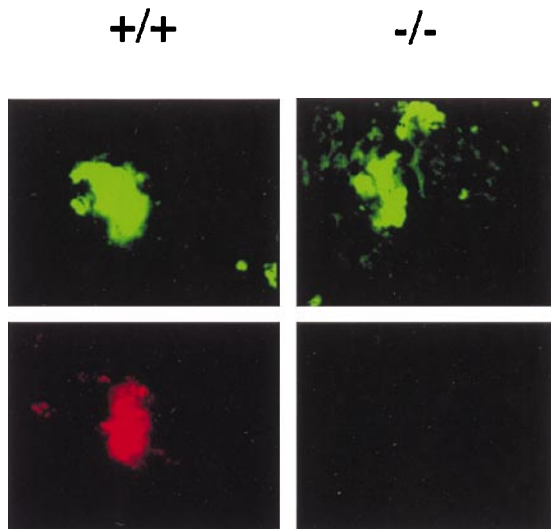

Fig. 6. *In vivo* interactions of intravenously injected tumor cells with platelets is P-selectin-dependent. Mice were intravenously injected with fluorescently labeled LS180 cells, and, after 30 min, frozen sections of the lungs were studied for the presence of tumors cells and associated platelets (anti-CD41) as described under *Materials and Methods*.

DISCUSSION

In many carcinomas, metastatic cells are enriched in sialylated Lewis blood group antigens (8, 10, 12, 25). Here we show that P-selectin, an endogenous lectin that can recognize sLe^x-containing mucins, is used by the tumor cells to promote their progression to the metastatic phenotype. The experimental metastasis assay indicates that P-selectin aids the colonization of hematogenously borne colon cancer cells in the lungs of the mice. The homing assay shows that this is partially because of improved initial seeding of cells into the lung. This hypothesis is strengthened by finding that mouse platelets interact with the carcinoma cell surface mucins in a P-selectin-dependent manner, both *in vitro* and *in vivo*. That the association occurs *in vivo* without the exogenous addition of thrombin indicates either that a subpopulation of circulating platelets is already expressing surface P-selectin, or that the tumor cells induce this expression, in cooperation with some other factors that are not present in the *in vitro* experiment. Regardless, the results support the notion that P-selectin-dependent formation of tumor:platelet clumps is a critical step in the process of metastasis formation. It does not, of course, rule out an additional role for P-selectin that might be expressed on the endothelial cells that make contact with tumor cells.

Unexpectedly, the primary flank tumors in P-selectin-deficient mice had a significantly slower growth rate. Occasional tumors even showed a partial regression and regrowth. This is particularly surprising because P-selectin is assumed to play a role in mediating extravasation of leukocytes into tissues and leukocytic infiltrates within tumors generally are inversely associated with tumor growth (46). Perhaps P-selectin does not play a dominant role in recruiting the chronic inflammatory infiltrate but has some other positive effect on tumor growth. Although others have suggested that sLe$^{x/a}$-containing glyco-conjugates may play a role in endothelial morphogenesis (47), we saw no obvious difference in the vascularization of tumors in P-selectin $-/-$ and P-selectin $+/+$ mice. It is more likely that P-selectin is involved in recruiting leukocytes and/or platelets that secrete growth factors and cytokines meant for wound healing—these might unwittingly stimulate the growth of tumor cells.

P-selectin ligands have been detected previously on several human carcinomas and cell lines (37, 39, 40) and hypothesized to play a role in metastasis. These data show that endogenous P-selectin can affect the *in vivo* behavior of tumor cells. Indeed, this information potentially can bring together several disparate observations about carcinomas: (*i*) the proposed role of platelets in facilitating tumor metastasis; (*ii*) the suggested importance of tumor microemboli-containing platelets and leukocytes in this process; (*iii*) Trousseau's syndrome, which occurs in patients with mucin-producing carcinomas and is associated with platelet-rich thrombemboli; (*iv*) the correlation of mucin production with poor clinical prognosis; and (*v*) the strong correlation of SLe^x expression with tumor progression, metastatic spread, and poor prognosis. Our data indicate that the common link may be P-selectin and its interactions with SLe^x-containing carcinoma mucins. We do not rule out additional roles for other selectins, because they also can recognize such mucins. Indeed, recent work from our lab indicates that each of the three selectins can have unique binding sites coexisting on a given carcinoma mucin molecule (Y.J.K., L.B., H. L. Han, N.M.V., and A.V., unpublished data). Because P-selectin can be coexpressed on the endothelium with E-selectin and both can recognize sLe^x antigens, both also could play a role in the homing of metastatic cells. However, only P-selectin provides a mechanistic connection involving platelets, which do not express L- or E-selectin.

One previous report showed that P-selectin recognizes sulfatides and theorized that the excretion of sulfatides might detach tumor cells from P-selectin-expressing cells such as the

endothelium (34). Although this hypothesis may apply in other circumstances, it is not consistent with the protective effect of P-selectin deficiency seen here. Our data also indicate that cancer mucins mediate direct interactions of circulating platelets with intravenously injected tumors cells. Thus, we envisage that large mucin molecules on the surface of tumor cells bearing multiple P-selectin-binding sites could bridge between tumor cells and P-selectin-expressing platelets and endothelium. The addition of leukocytes bearing PSGL-1 and/or L-selectin could favor the formation of the microemboli that are thought to aid the metastatic process (37).

In the final analysis, the precise mechanisms by which P-selectin facilitates tumor growth and progression remain to be defined. Regardless, we provide *in vivo* evidence that this cancer mucin–endogenous lectin interaction can have pathophysiological consequences. Because most relevant events occur and/or are initiated in the bloodstream, they are potentially amenable to intervention using anti-P-selectin therapeutics currently developed for modifying inflammatory and reperfusion injury states (31). In this regard, the clinically utilized antithrombotic agent heparin is a potent inhibitor of P-selectin binding to its natural ligand PSGL-1, at levels far lower than needed for its anticoagulant effects (48). Heparin and other sulfated compounds have been shown to block tumor metastases in some model systems (49–52), and mechanisms such as inhibition of heparanases, suppression of angiogenesis, and alteration of growth factor action have been suggested. Perhaps the ability of heparin to interfere with the interaction of P-selectin and tumor mucins also plays a major role in these antimetastatic effects.

1. Weiss, L. (1985) *Principles of Metastasis* (Academic, Orlando, FL).
2. Fidler, I. J. (1990) *Cancer Res.* **50,** 6130–6138.
3. Gasic, G. J. (1984) *Cancer Metastasis Rev.* **3,** 99–114.
4. Karpatkin, S. & Pearlstein, E. (1981) *Ann. Intern. Med.* **95,** 636–641.
5. Honn, K. V., Tang, D. G. & Crissman, J. D. (1992) *Cancer Metastasis Rev.* **11,** 325–351.
6. Toyoshima, M., Nakajima, M., Yamori, T. & Tsuruo, T. (1995) *Cancer Res.* **55,** 767–773.
7. Dennis, J. W. & Laferte, S. (1987) *Cancer Metastasis Rev.* **5,** 185–204.
8. Muramatsu, T. (1993) *Glycobiology* **3,** 291–296.
9. Fukuda, M. (1996) *Cancer Res.* **56,** 2237–2244.
10. Hakomori, S. (1996) *Cancer Res.* **56,** 5309–5318.
11. Kim, Y. S., Gum, J. & Brockhausen, I. (1996) *Glycoconjugate J.* **13,** 693–707.
12. Kim, Y. J. & Varki, A. (1997) *Glycoconjugate J.* **14,** 569–576.
13. McEver, R. P. (1997) *Glycoconjugate J.* **14,** 585–591.
14. Hilkens, J., Ligtenberg, M. J. L., Vos, H. L. & Litvinov, S. V. (1992) *Trends Biochem. Sci.* **17,** 359–363.
15. Ogata, S., Maimonis, P. J. & Itzkowitz, S. H. (1992) *Cancer Res.* **52,** 4741–4746.
16. Van de Wiel-van Kemenade, E., Ligtenberg, M. J. L., De Boer, A. J., Buijs, F., Vos, H. L., Melief, C. J. M., Hilkens, J. & Figdor, C. G. (1993) *J. Immunol.* **151,** 767–776.
17. Bresalier, R. S., Niv, Y., Byrd, J. C., Duh, Q. Y., Toribara, N. W., Rockwell, R. W., Dahiya, R. & Kim, Y. S. (1991) *J. Clin. Invest.* **87,** 1037–1045.
18. Hoff, S. D., Matsushita, Y., Ota, D. M., Cleary, K. R., Yamori, T., Hakomori, S. & Irimura, T. (1989) *Cancer Res.* **49,** 6883–6888.
19. Matsushita, Y., Cleary, K. R., Ota, D. M., Hoff, S. D. & Irimura, T. (1990) *Lab. Invest.* **63,** 780–791.
20. Matsusako, T., Muramatsu, H., Shirahama, T., Muramatsu, T. & Ohi, Y. (1991) *Biochem. Biophys. Res. Commun.* **181,** 1218–1222.
21. Sinn, H.-P., Brown, S. A., Oberle, E. & Thompson, J. S. (1992) *Int. J. Pancreatol.* **11,** 125–135.
22. Nakamori, S., Kameyama, M., Imaoka, S., Furukawa, H., Ishikawa, O., Sasaki, Y., Kabuto, T., Iwanaga, T., Matsushita, Y. & Irimura, T. (1993) *Cancer Res.* **53,** 3632–3637.
23. Nakayama, T., Watanabe, M., Katsumata, T., Teramoto, T. & Kitajima, M. (1995) *Cancer* **75,** 2051–2056.
24. Nakamori, S., Furukawa, H., Hiratsuka, M., Iwanaga, T., Imaoka, S., Ishikawa, O., Kabuto, T., Sasaki, Y., Kameyama, M., Ishiguro, S. & Irimura, T. (1997) *J. Clin. Oncol.* **15,** 816–825.
25. Kannagi, R. (1997) *Glycoconjugate J.* **14,** 577–584.
26. Izumi, Y., Taniuchi, Y., Tsuji, T., Smith, C. W., Nakamori, S., Fidler, I. J. & Irimura, T. (1995) *Exp. Cell Res.* **216,** 215–221.
27. Nakamori, S., Kameyama, M., Imaoka, S., Furukawa, H., Ishikawa, O., Sasaki, Y., Izumi, Y. & Irimura, T. (1997) *Dis. Colon Rectum* **40,** 420–431.
28. Springer, T. A. (1995) *Annu. Rev. Physiol.* **57,** 827–872.
29. Hynes, R. O. & Wagner, D. D. (1996) *J. Clin. Invest.* **98,** 2193–2195.
30. Kansas, G. S. (1996) *Blood* **88,** 3259–3287.
31. Lowe, J. B. & Ward, P. A. (1997) *J. Clin. Invest.* **99,** 822–826.
32. McEver, R. P. & Cummings, R. D. (1997) *J. Clin. Invest.* **100,** 485–492.
33. Varki, A. (1997) *J. Clin. Invest.* **99,** 158–162.
34. Aruffo, A., Kolanus, W., Walz, G., Fredman, P. & Seed, B. (1991) *Cell* **67,** 35–44.
35. Sawada, R., Tsuboi, S. & Fukuda, M. (1994) *J. Biol. Chem.* **269,** 1425–1431.
36. Miller, N., Vile, R. G. & Hart, I. R. (1996) *Glycoconjugate J.* **13,** 33–43.
37. Mannori, G., Crottet, P., Cecconi, O., Hanasaki, K., Aruffo, A., Nelson, R. M., Varki, A. & Bevilacqua, M. P. (1995) *Cancer Res.* **55,** 4425–4431.
38. Biancone, L., Araki, M., Araki, K., Vassalli, P. & Stamenkovic, I. (1996) *J. Exp. Med.* **183,** 581–587.
39. Aruffo, A., Dietsch, M. T., Wan, H., Hellström, K. E. & Hellström, I. (1992) *Proc. Natl. Acad. Sci. USA* **89,** 2292–2296.
40. Stone, J. P. & Wagner, D. D. (1993) *J. Clin. Invest.* **92,** 804–813.
41. Shinkai, Y., Rathbun, G., Lam, K. P., Oltz, E. M., Stewart, V., Mendelsohn, M., Charron, J., Datta, M., Young, F. & Stall, A. M. (1992) *Cell* **68,** 855–867.
42. Mayadas, T. N., Johnson, R. C., Rayburn, H., Hynes, R. O. & Wagner, D. D. (1993) *Cell* **74,** 541–554.
43. Hoshino, H., Tamaki, A. & Yagura, T. (1997) *Cell Struct. Funct.* **22,** 325–334.
44. McKenzie, B. A., Barrieux, A. & Varki, N. M. (1991) *Cancer Commun.* **3,** 15–19.
45. Baldini, A., Ross, M., Nizetic, D., Vatcheva, R., Lindsay, E. A., Lehrach, H. & Siniscalco, M. (1992) *Genomics* **14,** 181–184.
46. Kreider, J. W., Bartlett, G. L. & Butkiewicz, B. L. (1984) *Cancer Metastasis Rev.* **3,** 53–74.
47. Nguyen, M., Strubel, N. A. & Bischoff, J. (1993) *Nature (London)* **365,** 267–269.
48. Koenig, A., Norgard-Sumnicht, K., Linhardt, R. & Varki, A. (1998) *J. Clin. Invest.* **101,** 877–889.
49. Vlodavsky, I., Mohsen, M., Lider, O., Svahn, C. M., Ekre, H. P., Vigoda, M., Ishai-Michaeli, R. & Peretz, T. (1994) *Invasion Metastasis* **14,** 290–302.
50. Coombe, D. R., Parish, C. R., Ramshaw, I. A. & Snowden, J. M. (1987) *Int. J. Cancer* **39,** 82–88.
51. Lapierre, F., Holme, K., Lam, L., Tressler, R. J., Storm, N., Wee, J., Stack, R. J., Castellot, J. & Tyrrell, D. J. (1996) *Glycobiology* **6,** 355–366.
52. Sciumbata, T., Caretto, P., Pirovano, P., Pozzi, P., Cremonesi, P., Galimberti, G., Leoni, F. & Marcucci, F. (1996) *Invasion Metastasis* **16,** 132–143.